

# IMPROVED DATA OF SOLAR SPECTRAL IRRADIANCE FROM 0.33 TO 1.25 $\mu$ \*

HEINZ NECKEL

*Hamburger Sternwarte, Hamburg-Bergedorf, F.R.G.*

and

DIETRICH LABS

*Landessternwarte Königstuhl, Heidelberg, F.R.G.*

**Abstract.** The conversion of our centre of disk intensities published in 1968/70 into mean disk intensities has been repeated, using more accurate data for the centre-to-limb variation of both continuous radiation and strong absorption lines.

The random observational mean error of the new irradiance data very likely is not larger than 1.5% in the UV and not larger than 1% in the visible and infrared. Comparison with the fluxes of Sun-like stars observed by Hardorp (1980) confirms these errors and seems to exclude the possibility of a systematic, wavelength-dependent scale error which would correspond to a temperature difference larger than 50 K.

The resulting integral value of the irradiance between 0.33 and 1.25 $\mu$  is 1.060, the corresponding value of the solar constant lies between 1.368 and 1.377 kW m<sup>-2</sup>.

## 1. Introduction

With respect to the divers plans to search for *variations* in the solar irradiance, it may be profitable to have a base from which to start and which is as solid as possible. Therefore we do not hesitate to represent here improved data of the irradiance, even if hereby observations are involved, which were made nearly 20 years ago.

In the early 60's we measured absolute intensities at the centre of the solar disk in spectral bands 20.0/20.5 Å wide, using an almost rectangular apparatus profile. The corresponding intensity integrals we called  $\Sigma$  (Labs and Neckel, 1962, 1963, 1967):

$$\Sigma_i = \int_{\lambda_i - \Delta\lambda/2}^{\lambda_i + \Delta\lambda/2} I_\lambda d\lambda, \quad \begin{array}{l} \Delta\lambda = 20.5 \text{ \AA} \quad \text{for } \lambda_i \leq 4001.05 \text{ \AA}, \\ \Delta\lambda = 20.0 \text{ \AA} \quad \text{for } \lambda_i \geq 4020.0 \text{ \AA}. \end{array} \quad (1)$$

Later on (Labs and Neckel, 1968, 1970) we used these  $\Sigma$ -integrals to derive the corresponding integrals of the mean intensity ( $\phi$ ) and of the irradiance ( $\theta$ ), using the relations

$$\phi_i = \Sigma_i \frac{\phi_i}{\Sigma_i} = \Sigma_i \left( \frac{F}{I(0)} \right)_{\text{cont}} \left\{ \frac{1 - \eta_{\text{disk}}}{1 - \eta_{\text{centre}}} \right\}_i, \quad (2)$$

$$\theta_i = 6.800 \times 10^{-5} \phi_i. \quad (3)$$

$(F/I(0))_{\text{cont}}$  is the ratio of mean to central intensity as derived from centre-to-limb

\* Proceedings of the 14th ESLAB Symposium on *Physics of Solar Variations*, 16–19 September 1980, Scheveningen, The Netherlands.

observations of the continuous radiation (in UV of 'window'-intensities!), and the  $\eta$ 's are the line blocking coefficients for the 20 Å bands for disk-averaged radiation (irradiance) and central intensity, respectively.

Since Equation (2) has often been incorrectly interpreted, it should be emphasized, that it does *not* mean a simple derivation of the irradiance from a continuum-curve and line blocking data. The basic observed quantity  $\Sigma$  includes a priori all lines, and the third factor takes into account just the *centre to limb variation* of their strengths.

Most recently our irradiance data were used by Hardorp (1980) to compare them with the flux distribution of Sun-like stars. Thereby Hardorp found some differences between stellar and solar radiation, which demanded a clarification whether being real or not.

Therefore we checked the observed central intensities  $\Sigma$  as well as the data used to derive the corresponding irradiance values. With respect to the three factors forming the right-hand side of Equation (2), the result may be summarized as follows:

- (1) Our observed  $\Sigma$ 's are even more accurate than we have quoted so far.
- (2) For the ratio  $F/I(0)$  of mean to central intensity more reliable values are now derivable from the recent centre-to-limb observations of Pierce and Slaughter (1977a, b).
- (3) The former correcting factors taking into account the centre-to-limb variation of the  $\eta$ 's were erroneous for spectral bands with strong lines.

## 2. Random Errors of Central Intensity Integrals

While tests for possible *systematic* errors of our observations will be given in Sections 6 and 7, here we deal only with the *random* observational error, which can be inferred from the agreement of repeated observations, but also – and more conclusively – from the scatter around an appropriate smoothing curve.

Since the  $\Sigma$ 's themselves don't follow any smoothed curve if plotted against wavelength, the most objective way to exhibit their accuracy is to plot instead the resulting continuum intensities or the related radiation temperatures. This was done in Figure 1.

For  $\lambda < 0.66\mu$ ,  $T$  was derived from the window-intensities in  $\Sigma$ -calibrated atlases (Labs and Neckel, 1968, 1970, Table 5A), for  $\lambda > 0.66\mu$  from the quotients  $\Sigma/(1 - \eta_{\text{centre}})$ , where  $\eta_{\text{centre}}$  was either obtained from summation of the equivalent widths given by Moore *et al.* (1966) or – for  $\lambda > 0.877\mu$  – deduced from the atlas of Delbouille and Roland (1963). The occasional inclusion of terrestrial lines, which so far had been neglected, has now been taken into account. The resulting temperatures can be smoothed rather precisely by two r.m.s. parabolas:

$$\lambda \leq 3811.5 \text{ \AA} : T = 6206 + 238\,391 (\lambda - 0.3498)^2, \quad (4)$$

$$\lambda \geq 3999.9 \text{ \AA} : T = 6046 + 2\,021 (\lambda - 0.8699)^2. \quad (5)$$

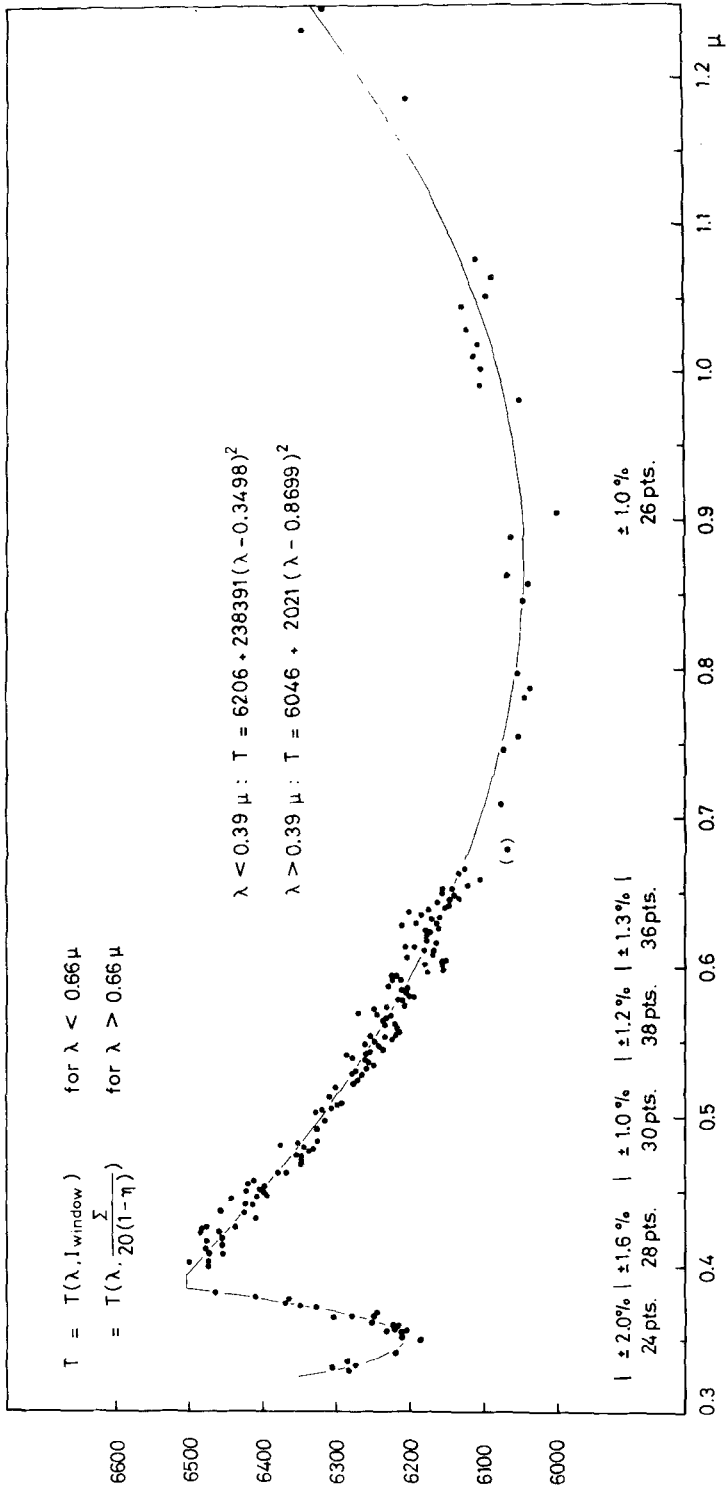


Fig. 1. Radiation temperatures of solar continuum as deduced from the  $\Sigma$ -integrals. The scatter around the second order r.m.s. curves yields just upper limits for the mean error of the  $\Sigma$ 's, because it includes not only the errors of the continuum derivation, but also the Sun's own departures from the adopted smoothing curves. The standard deviations of points within the marked spectral regions ( $\sqrt{[v\bar{v}]/n}$ ) refer to the intensities, not to the temperatures!

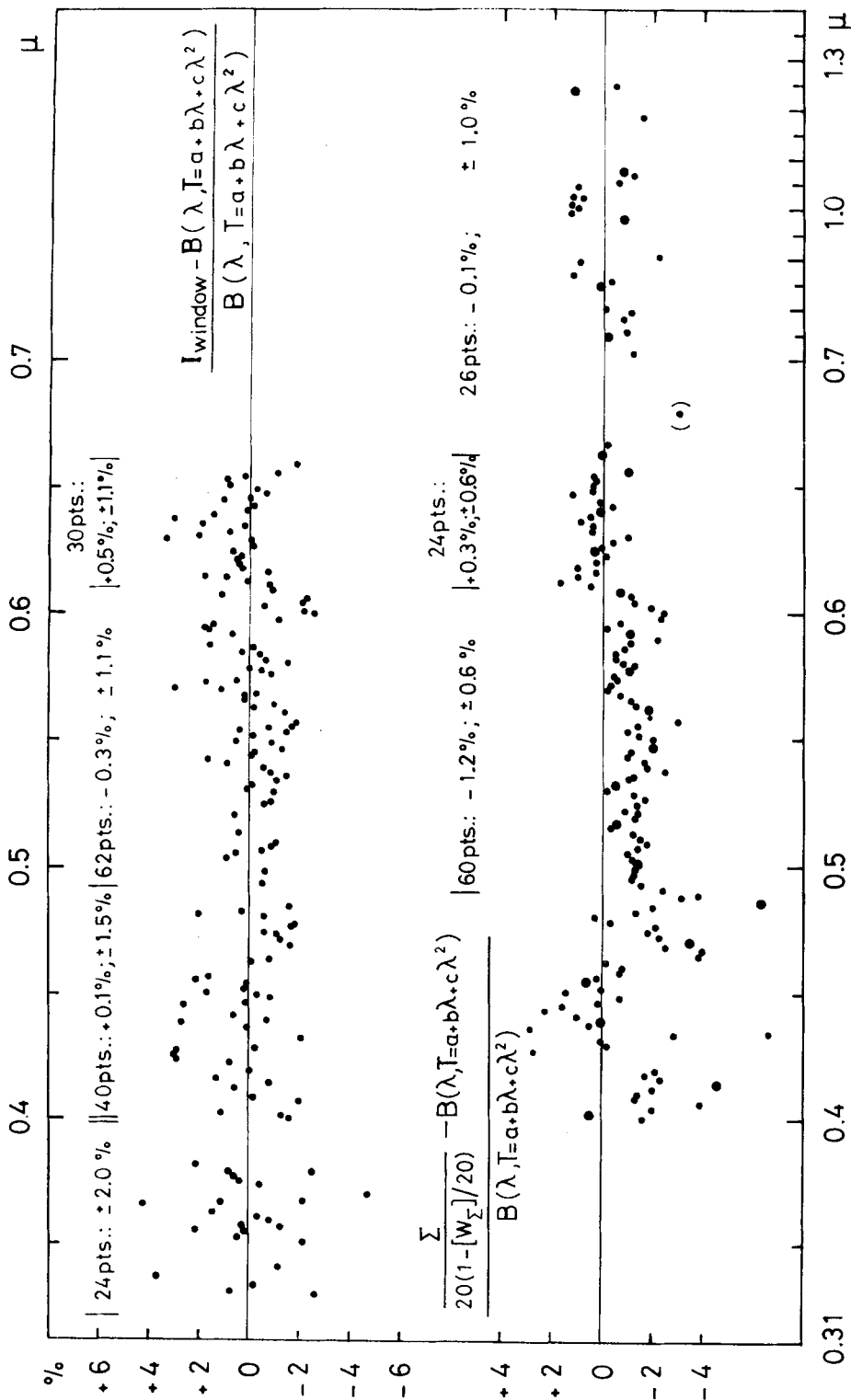


Fig. 2. Differences between 'observed' and computed (from Equations (4) and (5)) continuum in %. 'Observed' continuum in upper part; Window-intensities (Labs and Neckel, 1970, Table 5A) obtained from  $\Sigma$ -calibrated atlases; in lower part: Intensities resulting from the  $\Sigma$ 's, after correction for line absorption, which is taken here as the sum of equivalent widths of all lines included in the 20 Å-bands ( $= [W_{\Sigma}]$ ). For points within the marked spectral regions mean differences ( $[e_j]/n$ ) and standard deviations ( $\sqrt{[(v - \bar{v})^2]/(n - 1)}$ ) are given.

The corresponding standard deviations of the *intensities* are given at the bottom of the figure separately for 6 spectral subdivisions ( $\varepsilon = \sqrt{[vv]}/n$ ,  $n$  = number of points). They are – of course – only upper limits for the errors of the  $\Sigma$ 's: (1) They include for  $\lambda < 0.66\mu$  the errors of the atlas calibration and of the read-off of the window intensities as well as the intrinsic scatter of the window intensities, and for  $\lambda > 0.66\mu$  the errors of the equivalent widths; (2) very likely the r.m.s.-parabolas do not represent the real solar continuum.

The contribution of the window errors becomes evident in Figure 2. Here we plotted the deviations of the observed continuum intensities from the smoothed intensity curve, in the upper part for the window intensities (same value as in Figure 1), in the lower part for the values resulting from the  $\Sigma$ 's and the sum of equivalent widths (for  $\lambda > 0.66\mu$  same values as in Figure 1).

For wavelengths below  $H\beta$  the sum of the equivalent widths obviously does not yield reliable line blocking coefficients, but above  $H\beta$  the scatter is significantly smaller in the lower than in the upper part.

Disregarding the noticeable step at  $0.61\mu$ , below  $0.66\mu$  the scatter is characterized by a mean error of only  $\pm 0.6\%$ , but which still includes the errors of the equivalent widths. So it can be taken as a confirmation of the error derived for the average ratio  $\Sigma_{\odot}/(\Sigma_{\text{lamp}} \times \text{reflectivity of collimating mirror})$  obtained from repeated observations at the same wavelength: 0.3 to 0.7% in the visible and infrared (Labs and Neckel, 1967).

The reason for the step, which is detectable also in the upper part, could not be found. It may be due to a fault in our observations, or in the recordings of the Utrecht atlas, or may be a real feature.

After all it seems to be pretty sure, that at least in the visible and infrared the random observational error of the  $\Sigma$ 's is not larger and may be even smaller than  $\pm 1.0\%$ .

### 3. Ratio of Mean to Central Intensity for the Continuum

Next let us consider the situation for the second factor in Equation (2),  $(F/I(0))_{\text{cont}}$ . In Figure 3 we plotted the values which result from the centre-to-limb variations as observed by Pierce and Slaughter (1977a, b), as well as our former values, which were based mainly on the data published by David and Elste (1962). Since Pierce and Slaughter tabulated the coefficients for the fifth order fit of the CLV-curves,

$$I(\vartheta)/I(0) = A + B \cos \vartheta + C \cos^2 \vartheta + D \cos^3 \vartheta + E \cos^4 \vartheta + F \cos^5 \vartheta, \quad (6)$$

the corresponding  $F/I$ -ratios are easily obtained from

$$F/I = 2(A/2 + B/3 + C/4 + D/5 + E/6 + F/7). \quad (7)$$

Three types of differences are very obvious:

- (1) For shorter wavelengths the new data are systematically higher.

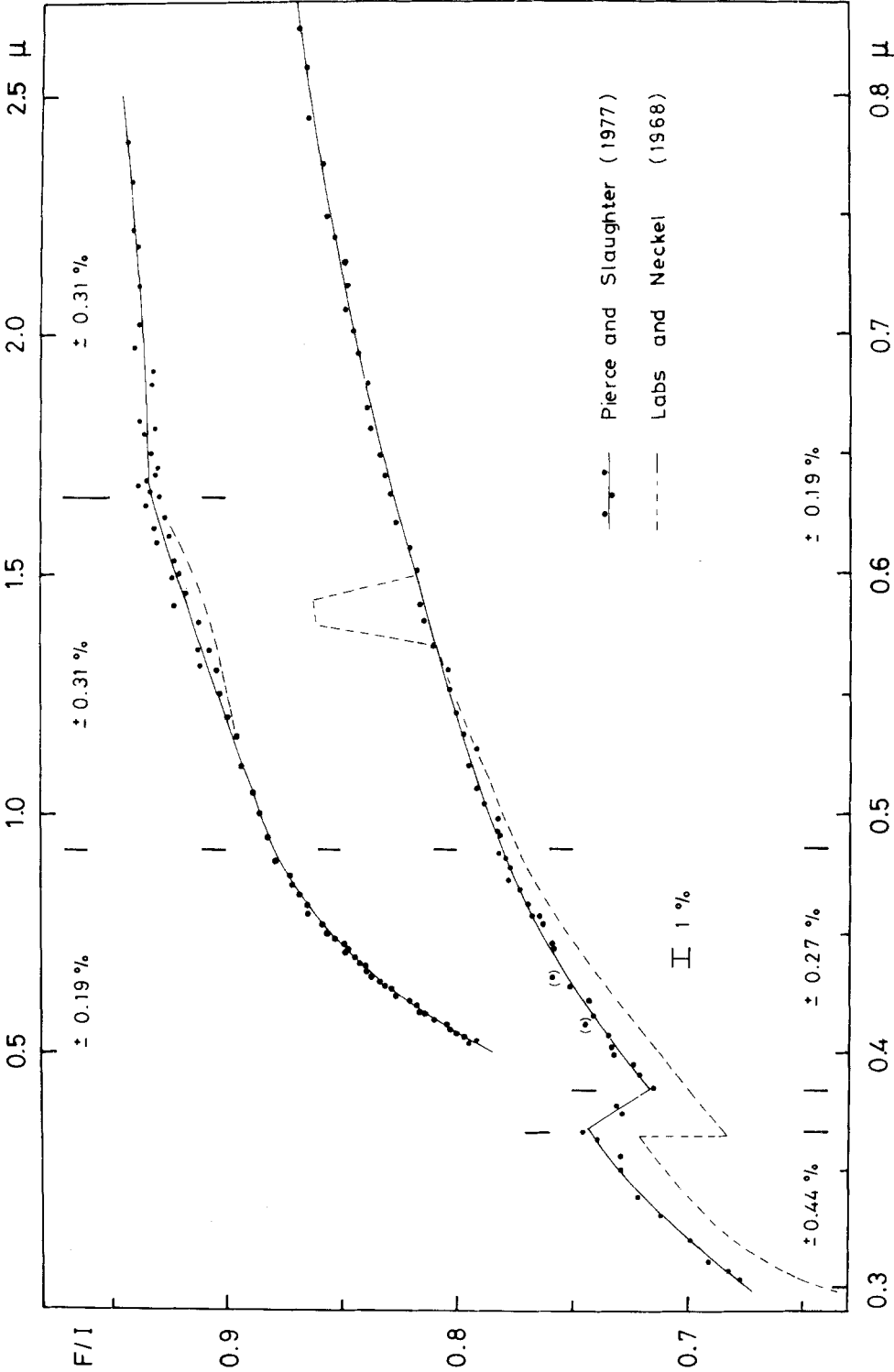


Fig. 3. Ratio of mean to central intensity for solar continuum (-windows). (1) Derived according to Equation (7) from the limb darkening data of Pierce and Slaughter (1977 a, b); (2) values which entered into our former derivation of solar irradiance (with two punching errors near  $\lambda = 0.59\mu$ ). The curves smoothing the data of Pierce and Slaughter are second order r.m.s. fits for the intervals marked by short vertical lines. The resulting standard deviations are given for each interval.

(2) Since in the vicinity of the Balmer limit no data had been available, we had adopted a much too ideal Balmer 'jump'.

(3) Between 0.57 and 0.60 $\mu$  the computer had been fed with faulty data due to incorrect punching. (Fortunately, this error has stolen just into Table 4 of our 1968 paper, but did not enter into any other data!)

For our new reduction, the proper  $F/I$ -values were taken from second order curves fitted to the new  $F/I$  data. The random errors of these r.m.s. curves are neglectable.

#### 4. Correction for Centre-to-Limb Variation of Fraunhofer Lines

The third and last factor in Equation (2),  $\{(1 - \eta_{\text{disk}})/(1 - \eta_{\text{centre}})\}_i$ , is the most problematic one. The plague is not the  $\eta_{\text{centre}}$  – it can be derived with high reliability for each of our spectral bands – but the corresponding  $\eta_{\text{disk}}$ . For its derivation we profited from the facts, that for many lines equivalent widths are known not only for the centre of the disk, but also for the limb region at  $\mu = \cos \vartheta = 0.3$ , and that the CLV of the line blocked radiation can be approximated with sufficient accuracy by

$$\eta_{\cos \vartheta} = \eta_{\text{centre}} + m(1 - \cos \vartheta). \quad (8)$$

Equation (8) implies that

$$\eta_{\text{disk}} - \eta_{\text{centre}} = k(\eta_{\mu=0.3} - \eta_{\text{centre}}), \quad (9)$$

where  $k$  does not depend on  $\eta_{\text{centre}}$  or  $m$  at all, but instead is a unique function of the limb darkening coefficients:

$$k = \frac{1}{1 - 0.3} \left( 1 - \frac{A/3 + B/4 + C/5 + D/6 + E/7 + F/8}{A/2 + B/3 + C/4 + D/5 + E/6 + F/7} \right), \quad (10)$$

$k$  increases from 0.38 at 0.33 $\mu$  to 0.44 at 1.25 $\mu$ .

In deriving our former irradiance tables, we had not only taken  $k$  as a constant (=0.6), but also had neglected that the fraction of radiation blocked by 'strong' lines  $\eta^s$  exhibits another CLV than the fraction  $\eta^n$  blocked by 'normal' lines, for which the average ratio  $\eta_{\mu=0.3}^n / \eta_{\text{centre}}^n$  is 1.05 (Labs and Neckel, 1968).

As a consequence, for bands affected by strong lines such as H and K of Ca II and the hydrogen lines – or their wings – the obtained irradiance data were wrong.

In our new reduction all significant strong lines, for which relevant data (CLV of profiles, wing intensities etc.) are available (David, 1961; de Jager, 1952; Allen, 1973), were separated from the bulk of the 'normal' lines and treated individually. For this procedure the third factor of Equation (2) has to be written – applying Equation (9) – as

$$\frac{1 - \eta_{\text{disk}}}{1 - \eta_{\text{centre}}} = 1 - k \frac{\eta_{\mu=0.3} - \eta_{\text{centre}}}{1 - \eta_{\text{centre}}} = 1 - k \frac{0.05 \eta_{\text{centre}}^n + s \eta_{\text{centre}}^s}{1 - (\eta_{\text{centre}}^n + \eta_{\text{centre}}^s)}, \quad (11)$$

where  $s = (\eta_{\mu=0.3}^s / \eta_{\text{centre}}^s) - 1$ . It usually was found to lie between the limits  $-0.68$  and  $+0.14$ . Only for bands, which are affected by the wings of the strong H-lines,  $s$  reaches  $-0.9$  or even  $-1.0$ .

The following strong lines could be taken into account:

H: $H\alpha$ to $H_{17}$ ,	Fe I:    d and $4045.8 \text{ \AA}$ ,
Na I: $D_1$ and $D_2$ ,	Ca I:    g,
Mg I: $b_1, b_2, b_4$ ,	Ca II:    H and K.

The line blocking coefficients  $\eta_{\text{centre}}^n$ , but which enter into Equation (11) only with a rather low weight, were counted correctly from the level of the 'quasi-continuum' (r.m.s.-curves in Figure 1) as it is defined by the intensities of the windows, to which also the  $(F/I)_{\text{cont}}$ -data refer (and not from the 'true' or model continuum as in our previous reduction).

For  $\lambda < 0.61\mu$ ,  $\eta_{\text{centre}}^n$  was obtained from

$$\eta_{\text{centre}}^n = \eta_{\text{centre}} - \eta_{\text{centre}}^s = \left(1 - \frac{\Sigma}{20I_{\text{cont}}}\right) - \eta_{\text{centre}}^s, \quad (12)$$

for  $\lambda > 0.61\mu$  it was taken as the sum of equivalent widths, divided by 20.

The resulting ratios of mean to central intensity for our  $20 \text{ \AA}$  bands are shown in Figure 4 for the region from  $0.35$  to  $0.45\mu$ . In this range they can be compared with a detailed  $F/I$ -curve, which is deducible from a figure published by Canavaggia and Chalonge (1946), giving  $\log(I_{0.9}/I_{0.0})$ .

Judging the agreement, the following facts must be considered:

- (1) The curve results from photographic photometry.
- (2) Left of the interruption near  $0.39\mu$ , the reconstructed curve became too low by 1 to 2%, which is evident from comparison with the continuum values given by Canavaggia and Chalonge themselves as well as by Pierce and Slaughter.
- (3) In the centres of the Ca II H- and K-lines no points were given by Canavaggia and Chalonge. It seems, that the points in the wings of these lines should not have been connected.

Longward of  $0.40\mu$  the agreement is almost perfect, except for the one spectral band centered at  $0.4306\mu$ . It is a band with exceptional strong absorption (46%), which is to a large extent caused by CH and  $\text{CH}^-$ . We conclude, that these lines don't show the average increase but actually decrease towards the limb.

### The Final Irradiance Data

A compilation of the new irradiance data is given in Tables II–IV at the end of this paper. Figure 5 gives the ratio of new (Table II) to old (Labs and Neckel, 1968, Table 4, but with Labs and Neckel (1970) corrections) values, plotted against wavelength. It summarizes synoptically all improvements:

- (1) The general increase towards shorter wavelengths is due to the new limb darkening data of Pierce and Slaughter.



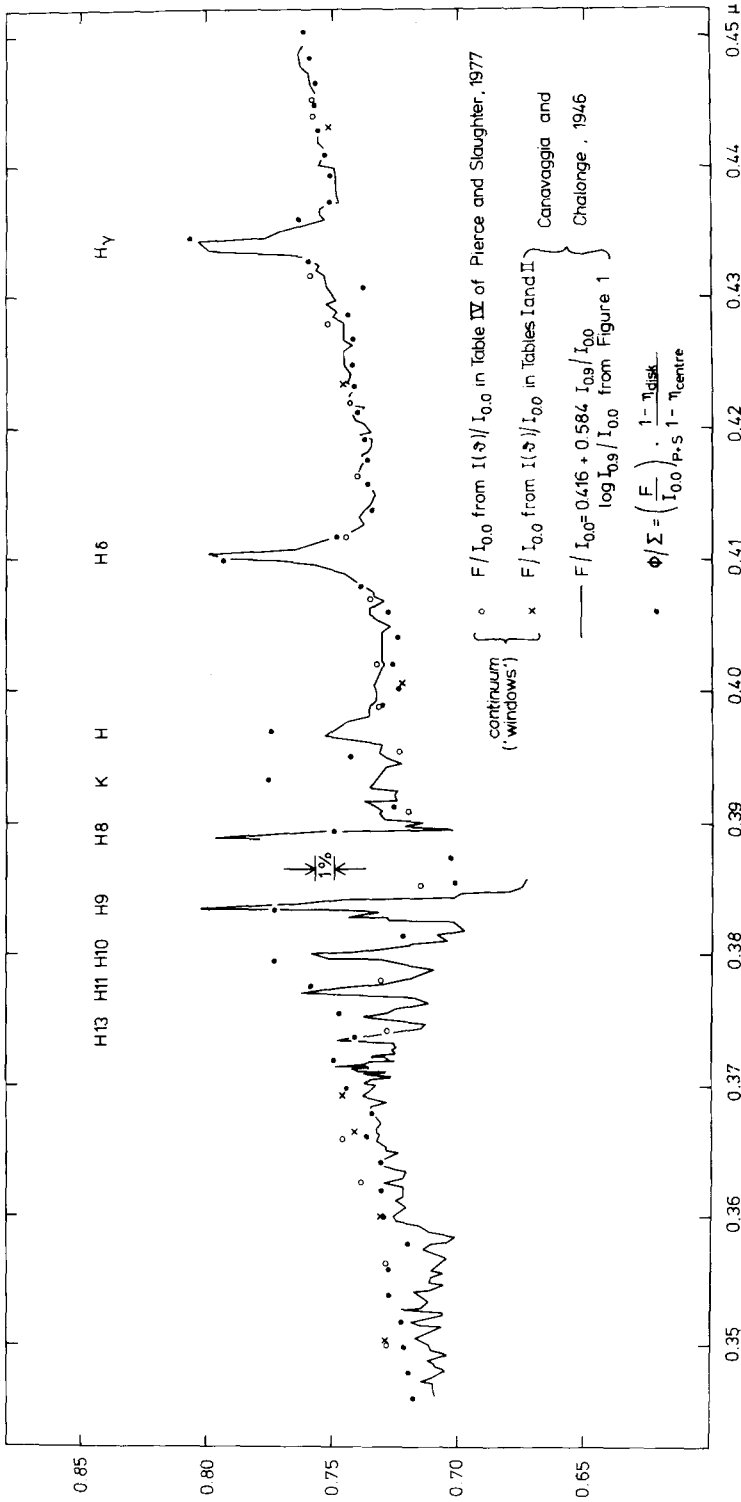


Fig. 4. Ratios of mean to central intensity. (1) For the continuum (-windows) as adopted in this paper (circles). (2) For continuum (-windows) according to limb darkening curves obtained - within the same experiment as below - from photographic spectra for 9 points along the solar radius (crosses). (3) Deduction from a figure giving  $\log(I_{0,9}/I_{0,0})$ , which was constructed from microphotometer tracings of photographic spectra taken at centre and limb ( $\sin \theta = 0.9$ ) of solar disk (curve). (4) For our 20 Å spectral bands as deduced from the corresponding continuum values and the available data about the CLV of lines (points).

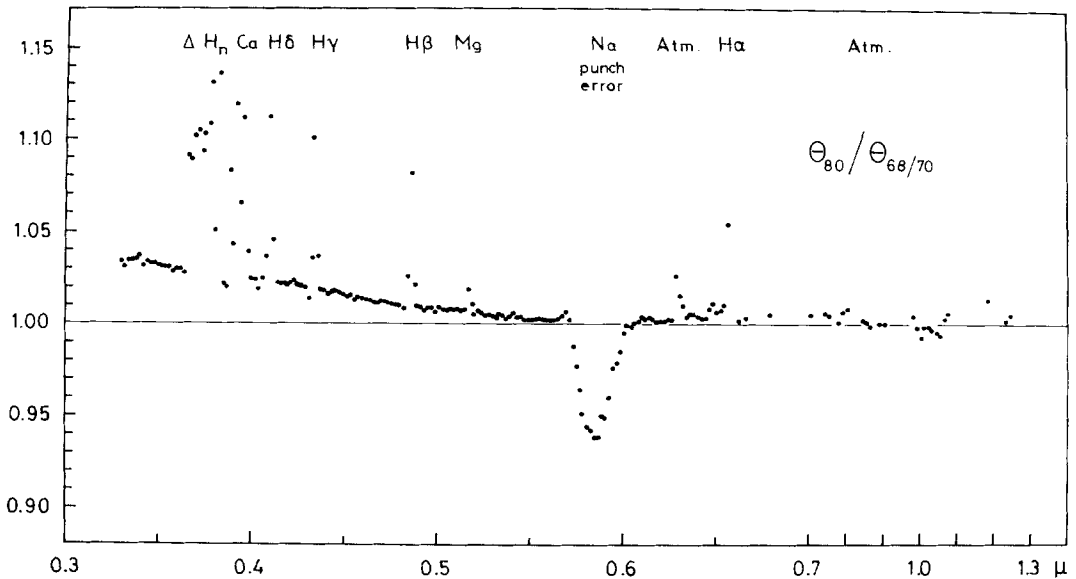


Fig. 5. Ratio of 20 Å irradiance integrals evaluated in this paper to the former values, which were given in Table 4 of Labs and Neckel (1968), corrected for new radiation constants (Labs and Neckel, 1970). The reasons for the largest corrections are indicated at the top. They don't need to be explained except for the following ones:  $\Delta$ : Formerly incorrect Balmer 'jump';  $H_n$ : Hydrogen-lines  $H_\delta$  to  $H_{17}$ ; Atm.: Lines originating in the Earth's atmosphere.

(2) Nearly all deviations from a smoothed curve are due to taking now into account the abnormal centre-to-limb variation of the strongest lines, but near the Balmer limit they are due to our formerly incorrect Balmer jump in the  $(F/I)_{\text{cont}}$ -curve.

(3) The dip around  $0.59\mu$  arises from two errors in punching the old  $(F/I)_{\text{cont}}$ -data (see remark in Section 3, point (3)).

(4) At some wavelengths, especially around  $0.63\mu$  and in the infrared, the corrections concern the  $\Sigma$ 's themselves. These – mostly rather small – corrections are due to the occasional inclusion of terrestrial lines, which so far had been neglected.

The significance and reliability of these improvements become evident in Figure 6, which we have adopted from Hardorp's work, but supplemented by our new data.

This interesting figure gives the magnitude differences  $\Delta m$  between published irradiance data and the deflections in daylight-recordings for 20 Å bands obtained by Hardorp, but with the slope tilted by multiplication with  $\lambda^4$  (N.B.:  $\Delta m = 2.5 \log (\text{Irr}_{\text{Sun}}/\text{Defl}_{\text{sky}})$ ) and arbitrary constants added.

From the four zigzag lines let us consider only the two lowest ones. The continuous course corresponds to our former, the dashed course to our new irradiance data. Very obviously, with the new data the scatter is significantly smaller. From the remaining scatter, but which includes also the errors of the sky observations

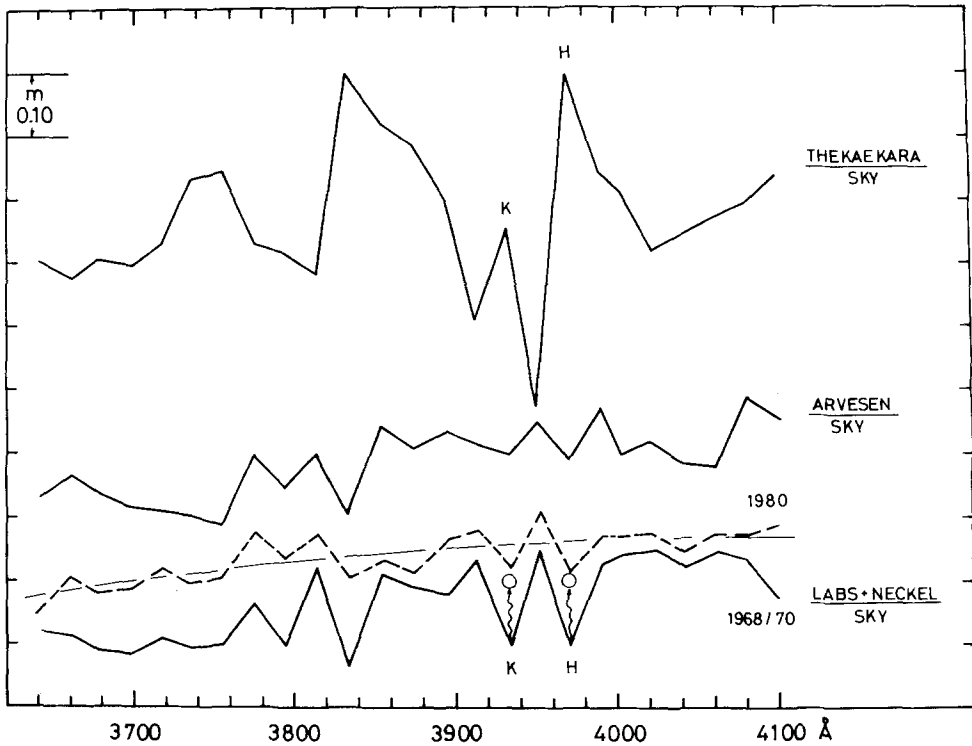


Fig. 6. Comparison between solar irradiance data and uncalibrated scans of the daylight sky, adopted from Hardorp (1980), but with our new data added (dashed zigzag line and corresponding smoothing curve). Given are the 'magnitude'-differences  $\Delta m$ , multiplied by  $\lambda^4$  and with different arbitrary constants added.  $\Delta m = 0''10$  corresponds about to 9.7% ( $\Delta m = 2.5$  log intensity-ratio).

(compare with Arvesen's curve!), one must conclude, that even in this critical region the random mean error of our irradiance data is not larger than 1.5%. So we feel sure, that the accuracy of the new irradiance is not significantly worse than that of the central intensities.

## 6. Comparison with Sun-like Stars Observed by Hardorp

Good evidence, that our irradiance data are basically free from a severe systematic error as far as a *wavelength-dependent* scale factor is concerned, comes from Hardorp's observations of Sun-like stars.

According to him, the two main sequence stars 16 Cyg B and Hyades 64 are the best 'solar analogs' (so far found), because of the close agreement of spectral, temperature-sensitive spectral features in the UV, which indicate nearly identical temperatures.

It was Hardorp's comparison of the fluxes of these stars with our solar irradiance, which revealed those anomalies, which stimulated this new reduction. We will repeat here his comparison, but using our new data.

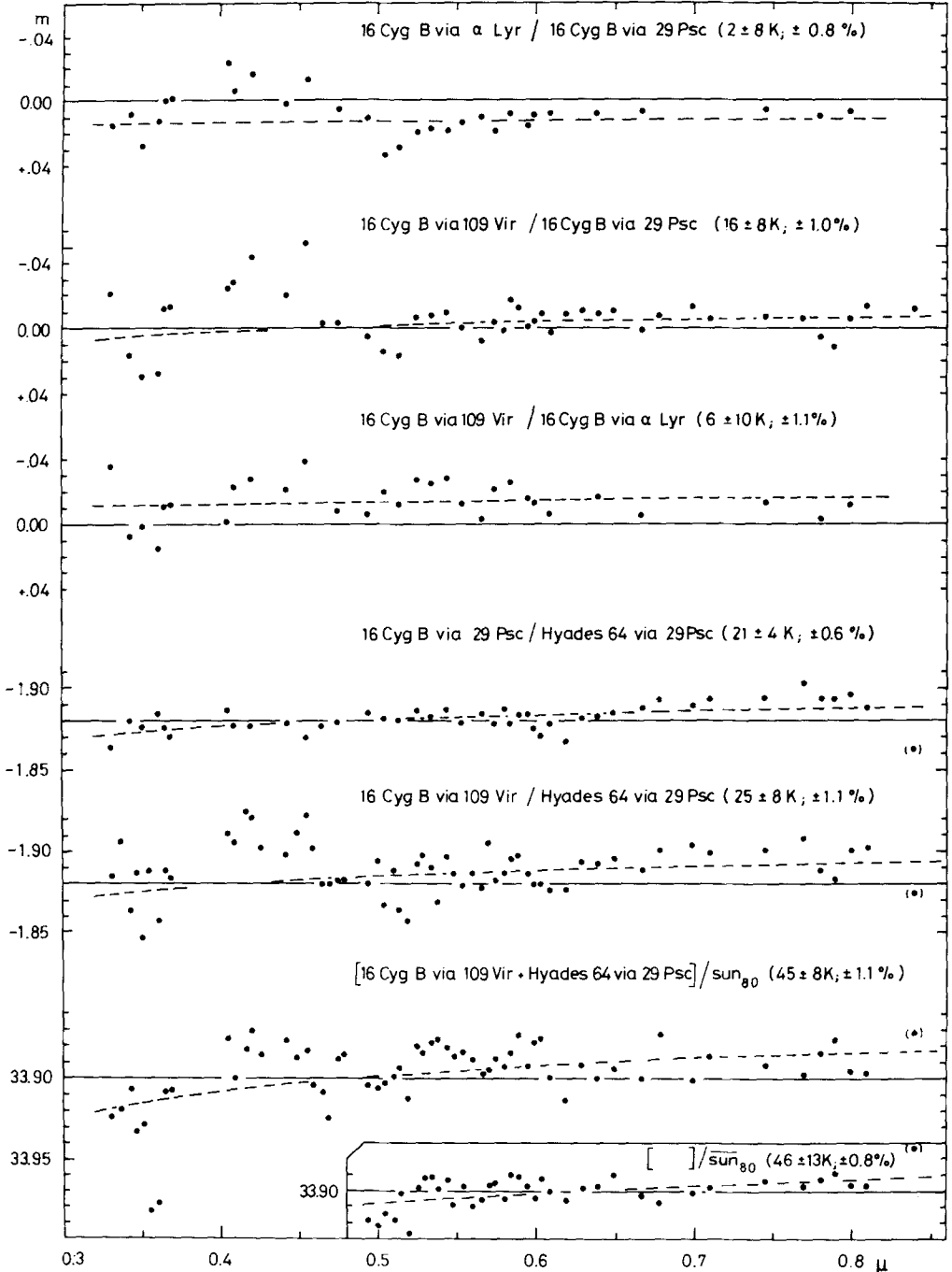


Fig. 7. Comparison between different calibrations of the two Sun-like stars 16 Cyg B and Hyades 64 as well as between mean stellar flux and solar irradiance (for  $\lambda > 0.5\mu$  also for solar data obtained from smoothed continuum). The points give the 'magnitude'-differences  $\Delta m$  for Hardorp's 40 Å spectral bands ( $\Delta m = 0^m.01$  corresponds to about 0.93% in intensity). r.m.s. fits of curves being proportional to  $1/\lambda$  yield the temperature differences and standard deviations (in % of observed intensity) given in brackets. For these fits the points between 0.40 and 0.46 $\mu$  have been excluded, if one of the standard stars  $\alpha$ Lyr or 109 Vir is involved. The same holds for the two points at 0.355 and 0.361 $\mu$  in the comparison with the Sun.

Hardorp obtained the fluxes of the Sun-like stars by comparison with three absolutely calibrated standard stars, namely  $\alpha$ Lyr, 109 Vir, and 29 Psc. His observations were made in 40 Å bands, which agree with two adjacent ones of our 20 Å bands.

In Figure 7, the three upper sets are plotted to give some idea about the accuracy of the fluxes of the standard stars. Here we compare – again in a ‘magnitude’-scale – the fluxes of 16 Cyg B as obtained by using different standard stars. The dashed lines represent  $1/\lambda$ -gradients obtained by r.m.s. fits; the corresponding temperature differences and the resulting standard deviations are given in brackets.

The next set shows the comparison of both Sun-like stars, if their fluxes are obtained via the same standard star (29 Psc). So all errors of the absolute calibration cancel out and we see, how closely the fluxes of these stars actually agree.

The 5th set shows again the comparison of both Sun-like stars, but after calibration with different standard stars, and the 6th set finally the comparison between the mean of both stellar calibrations and the solar irradiance. Figure 8 shows further Sun-star comparisons.

For  $\lambda > 0.5\mu$  it is also shown, how the comparisons look like, if the solar irradiance is obtained from the smoothing curve for the continuum-temperatures (compare Figure 1) and the line-blocking coefficients resulting from summing-up the equivalent-widths.

From all comparisons one must conclude, that the Sun in fact does agree as good with the stars as the stars with each other. Two anomalies should be mentioned:

(1) Between 0.40 and 0.46 $\mu$  slight differences remain, if  $\alpha$ Lyr or 109 Vir serve as the standard star, but are not present, if the two Sun-like stars are related to 29 Psc.

(2) In all star-Sun comparisons two points near 0.36 $\mu$  depart severely, very likely because of an abnormal centre-to-limb variation of the most relevant lines.

For the r.m.s. fits those anomalous points have been excluded. Please note, that the standard deviations given in Figures 7 and 8 for the Sun/star comparisons (1.1 or 1.2%) include – of course – the errors of the solar irradiance as well as those of the stellar fluxes. So these comparisons confirm, that the mean error of our irradiance can not be larger but very likely is slightly smaller than 1.0%.

Slight differences in temperature are indicated in the sense, that both stars are cooler than the Sun, Hyades 64 by about 30 K and 16 Cyg B by about 50 K. The question, whether these differences are real or due to systematic errors in the stellar and/or solar data can not be answered. So these differences can be taken as the upper limits of a systematic error in the solar irradiance. In this connection it should be pointed out, that 50 K correspond to about half a spectral subclass, and that the spectral types of both Sun-like stars are G5 V! The associated problems have been discussed by Hardorp.

## 7. The Resulting Solar Constant

In Table I we give the irradiance-integrals, which follow from our observations, separately for three subdivisions:

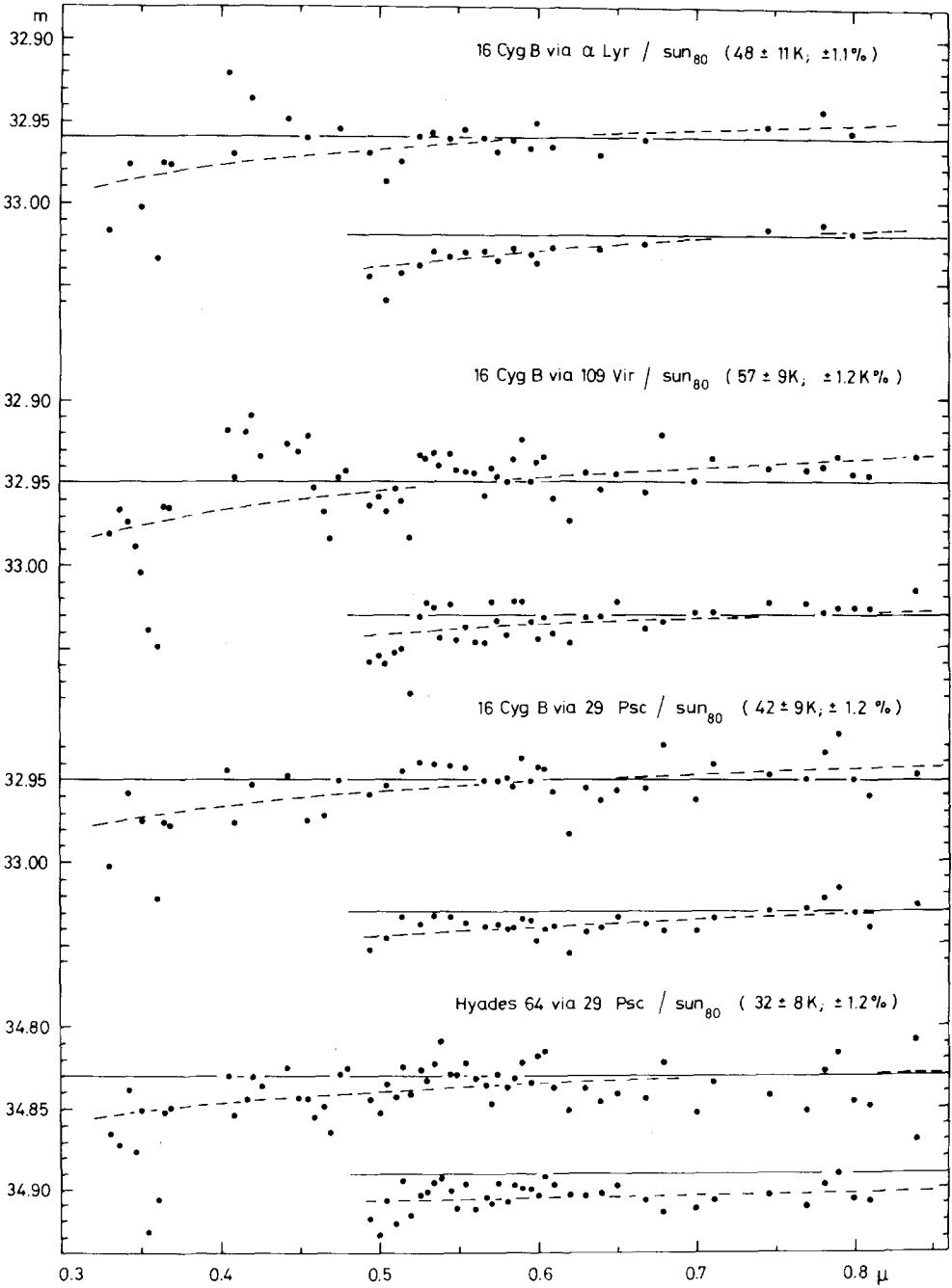


Fig. 8. Further comparisons of solar irradiance with the fluxes of 16 Cyg B and Hyades 64. For details see caption of Figure 7.

TABLE I  
Integral values of solar spectral irradiance in  $\text{kW m}^{-2}$

0.1510–0.2100 $\mu$	a: Donnelly and Pope (1973) b: Samain and Simon (1976)	0.000 2 0.000 2
0.2100–0.3000 $\mu$	a: Donnelly and Pope (1973) b: Broadfoot (1972)	0.016 0 0.016 2
0.3000–0.3300 $\mu$	a: Tousey (1963) ( $\times 0.844$ ) b: Arvesen <i>et al.</i> (1969)	0.020 8 0.022 0
0.3300–0.6569 $\mu$		0.540 3
0.6569–0.8770 $\mu$		0.272 0
0.8770–1.25 $\mu$	a: $\eta = 2.0\%$ b: $\eta = 1.0\%$	0.246 4 0.248 9
1.25–2.5 $\mu$	a: Pierce (1954)/Labs and Neckel (1968/70) b: Arvesen <i>et al.</i> (1969)	0.225 7 0.228 9
2.5–10 $\mu$	a: Several authors/Labs and Neckel (1968/70) b: Thekaekara (1970)	0.045 6 0.047 9
>10 $\mu$	Mankin (1977)	0.000 8
	Total	a: 1.368 b: 1.377

(1) The region 0.3300 to 0.6569 $\mu$  is completely covered by our spectral bands; here we had just to add the  $\theta$ -integrals, taking into account overlapping areas.

(2) From 0.6569 to 0.8770 $\mu$  the  $\theta$ -integrals had to be computed from the interpolation formula for the continuum temperatures (Equation (5)), the  $(F/I)_{\text{cont}}$ -values and the line-blocking obtained from summing-up the equivalent widths (Table III).

(3) Above 0.8770 $\mu$  no reliable absorption data are available. Therefore we made two assumptions:  $\eta = 1\%$  and  $\eta = 2\%$ . The true value should be somewhere between these limits. The *continuum* integrals are given in Table IV.

For the regions outside the range observed by us we adopted the irradiance from the literature as indicated.

Adding all the smallest and all the largest values yields the limits of the solar constant. The exact agreement of the mean value with that one proposed by Fröhlich (1977),  $S = 1.373 \text{ kW m}^{-2}$ , indicates, that – by chance – our irradiance does also not suffer from any noticeable *neutral* scale error.

## 8. Concluding Remarks

It seems that the irradiance data given in Tables II to IV are the most reliable ones available at present. However, some uncertainties remain, due to our incomplete

TABLE II

Solar irradiance  $\theta_{20}(\mu\text{W cm}^{-2})$  for 20.0 Å (for  $\lambda \leq 4001.5 \text{ Å} : 20.5 \text{ Å}$ ) bands according to observed intensity integrals which include all lines ( $\lambda = \text{centre of band}$ . Partly overlap!)

$\lambda$	$\theta_{20}$	$\lambda$	$\theta_{20}$	$\lambda$	$\theta_{20}$	$\lambda$	$\theta_{20}$
3298.15	215.3	4267.9	324.0	5219.3	376.2	6200.0	343.0
3317.65	197.4	4286.4	329.8	5238.8	382.7	6219.7	338.1
3337.95	190.0	4306.4	246.0	5258.0	366.3	6239.0	331.4
3358.55	182.0	4326.4	358.7	5278.0	361.6	6259.0	331.6
3378.65	177.9	4339.7	347.3	5298.0	388.2	6279.0	336.3
3398.25	201.7	4359.2	371.1	5316.5	386.8	6299.0	328.0
3418.65	191.5	4371.9	368.7	5335.2	368.7	6319.0	330.0
3437.95	175.7	4391.9	334.7	5353.9	387.5	6339.0	328.3
3458.25	188.8	4409.0	358.7	5372.0	369.9	6359.0	331.4
3478.55	190.8	4428.0	391.1	5391.5	368.5	6379.0	332.5
3498.15	196.8	4447.2	389.6	5410.0	361.0	6399.0	324.1
3518.55	194.6	4464.0	370.3	5430.0	370.9	6419.0	321.9
3538.95	231.1	4483.2	404.0	5450.0	377.5	6439.0	324.0
3559.05	216.0	4503.2	426.0	5470.0	368.7	6459.0	322.4
3579.35	152.6	4523.6	399.3	5490.0	373.5	6479.0	322.4
3599.55	217.7	4543.6	402.6	5508.0	371.6	6499.0	312.9
3620.15	213.8	4563.6	411.8	5527.3	370.7	6519.0	320.4
3640.55	203.2	4583.7	403.2	5547.0	376.2	6539.0	318.1
3661.05	257.6	4603.7	404.3	5566.9	360.1	6559.0	274.6
3677.75	235.7	4623.6	418.9	5586.9	359.9	6621.0	314.9
3698.25	246.1	4643.6	398.9	5606.9	360.8	6663.0	310.0
3718.65	238.0	4663.6	391.3	5626.9	370.7	6790.0	293.9
3736.65	196.9	4683.5	402.2	5646.0	365.8	7090.0	276.0
3754.75	209.4	4703.5	388.6	5666.0	364.4	7465.0	257.4
3775.25	278.0	4723.3	403.7	5686.0	367.4	7552.0	250.3
3794.35	245.9	4743.3	406.4	5706.0	357.8	7815.0	237.4
3813.95	229.6	4763.3	394.4	5726.0	374.5	7875.0	233.6
3833.55	149.8	4783.3	410.1	5746.0	368.5	7980.0	230.1
3853.75	206.1	4803.3	412.8	5766.0	368.3	8465.0	204.9
3873.75	199.8	4823.3	408.3	5784.5	360.5	8570.0	200.8
3894.15	234.6	4843.1	402.4	5804.5	368.0	8633.0	201.4
3911.95	259.9	4863.1	343.0	5824.5	368.8	8880.0	189.9
3932.45	153.1	4883.1	375.5	5844.5	366.6	9042.0	177.8
3950.25	260.2	4892.9	387.9	5864.5	357.9	9815.0	152.8
3969.25	177.3	4912.9	376.8	5884.0	349.0	9904.0	152.7
3989.25	321.2	4932.9	387.0	5903.7	347.7	10010.0	149.1
4001.05	340.3	4951.5	397.8	5923.5	355.3	10100.0	147.0
4020.00	357.1	4970.7	398.7	5943.5	357.4	10179.0	144.0
4040.00	324.4	4988.9	384.2	5963.5	359.2	10270.0	141.8
4060.00	329.1	5008.9	364.7	5983.0	346.3	10440.0	136.6
4078.80	338.3	5028.9	384.4	6003.0	344.9	10510.0	132.5
4098.80	332.0	5048.9	383.1	6023.0	341.1	10640.0	128.6
4117.10	362.7	5068.3	393.4	6043.0	351.7	10768.0	126.0
4137.10	346.6	5088.3	385.5	6063.0	347.4	11860.0	101.8
4156.50	357.7	5108.3	386.4	6080.0	346.0	12330.0	96.7



Table II (continued)

$\lambda$	$\theta_{20}$	$\lambda$	$\theta_{20}$	$\lambda$	$\theta_{20}$	$\lambda$	$\theta_{20}$
4175.90	338.5	5128.3	379.0	6100.0	344.0	12470.0	93.0
4191.20	331.2	5148.3	370.5	6120.0	347.6		
4211.20	363.7	5168.3	338.4	6140.0	339.9		
4231.00	330.0	5188.3	346.6	6160.0	333.8		
4247.50	350.2	5199.5	363.6	6180.0	345.0		

TABLE III

Solar irradiance  $\theta_{50}(\mu\text{W cm}^{-2})$  for 50 Å bands between 6569 and 8770 Å. From smoothed continuum (Figure 1; Equation (5)) and line blocking data ( $\lambda =$  centre of band)

$\lambda$	$\theta_{50}$	$\lambda$	$\theta_{50}$	$\lambda$	$\theta_{50}$	$\lambda$	$\theta_{50}$
A6584.5	484.3	7125	693.1	7725	604.1	8325	524.0
		7175	680.3	7775	601.3	8375	523.4
6625	781.0	7225	674.7	7825	593.9	8425	515.8
6675	775.1	7275	669.2	7875	591.3	8475	498.8
6725	761.2	7325	663.7	7925	574.4	8525	471.2
6775	757.2	7375	648.2	7975	574.5	8575	499.3
6825	746.4	7425	635.8	8025	566.3	8625	493.9
6875	738.3	7475	641.3	8075	557.0	8675	462.3
6925	731.9	7525	632.5	8125	557.4	8725	479.3
6975	722.0	7575	627.4	8175	544.6		
7025	704.7	7625	625.7	8225	537.9	B8760	191.0
7075	704.8	7675	604.3	8275	538.0		

A) Bandwidth = 31 Å.

B) Bandwidth = 20 Å.

TABLE IV

Solar irradiance  $\theta_{100}(\mu\text{W cm}^{-2})$  for 100 Å bands between 8770 and 12500 Å. Smoothed continuum values according to Figure 1 and Equation (5) (No lines included!  $\lambda =$  centre of band)

$\lambda$	$\theta_{100}$	$\lambda$	$\theta_{100}$	$\lambda$	$\theta_{100}$	$\lambda$	$\theta_{100}$
A8785	289.8	9550	816.3	10550	663.7	11550	549.1
		9650	798.9	10650	650.7	11650	539.3
		9750	782.1	10750	638.1	11750	529.8
8850	952.2	9850	765.7	10850	625.9	11850	520.5
8950	931.1	9950	749.8	10950	614.0	11950	511.4
9050	910.5	10050	734.4	11050	602.4	12050	502.6
9150	890.5	10150	719.4	11150	591.1	12150	494.0
9250	871.5	10250	704.9	11250	580.2	12250	485.7
9350	852.5	10350	690.7	11350	569.5	12350	477.5
9450	834.1	10450	677.0	11450	559.2	12450	469.6

A) Bandwidth = 30 Å.

knowledge of the centre-to-limb variation of the absorption lines. In this sense we consider the improvements given as preliminary only.

Therefore we do intend observations of the CLV of all our 20 Å spectral bands, for which we have measured the intensity integral  $\Sigma$  at the centre of the disk. Such observations would yield immediately and with high reliability the ratio  $\phi/\Sigma$ , so that the only errors of the resulting irradiance integrals  $\theta$  would be just those of the  $\Sigma$ 's.

Even with respect to the intended high precision for the planned irradiance measurements, this procedure seems to be justified:

(1) The accuracy of the  $\Sigma$ 's is well established, but not yet that one of the planned irradiance observations.

(2) In any case the relation  $\phi = \Sigma(\phi/\Sigma)$ , which must be fulfilled *exactly* by the observations, provides a unique possibility to test reliability and consistency of the three independently observable quantities  $\phi$ ,  $\Sigma$ , and  $\phi/\Sigma$ .

Finally, one should not forget, that information about the probability, that the solar irradiance is variable, may be obtained also from observations of Sun-like stars. As far as we know, no such star is known at present to be a variable. Long term observations of selected G-type stars, which can be done for wavelengths observable from the ground by comparison with other stars with high precision ( $\pm 0.1\%$ ), could yield valuable hints concerning the variations one should expect for the Sun.

### Acknowledgement

We are indebted very much to J. Hardorp for sending us a preprint of his paper and the table with the energy distribution of Hyades 64 via 29 Psc, so giving us the opportunity to use his data prior to final publication.

### References

- Arvesen, J. C., Griffin, N. R., Jr., and Pearson, B. D.: 1969, *Appl. Opt.* **8**, 2215.  
 Broadfoot, A. L.: 1972, *Astrophys. J.* **173**, 681.  
 Canavaggia, R. and Chalonge, D.: 1946, *Ann. Astrophys.* **9**, 143.  
 David, K. H.: 1961, *Z. Astrophys.* **53**, 37.  
 David, K. H. and Elste, G.: 1962, *Z. Astrophys.* **54**, 12.  
 de Jager, C.: 1952, *Rech. Utrecht XIII*, Part 1.  
 Delboille, L. and Roland, G.: 1963, *Photometric Atlas of the Solar Spectrum from 7498 to 12 016 Å*, Astrophys. Inst. of the Univ. Liège.  
 Donnelly, R. F. and Pope, J. H.: 1973, NOAA Techn. Report ERL 276-SEL 25, U.S. Government Printing Office, Washington, D.C.  
 Fröhlich, C.: 1977, in *The Solar Output and its Variation*, Colorado Assoc. Univ. Press, Boulder, p. 93.  
 Hardorp, J.: 1980, *Astron. Astrophys.* **91**, 221.  
 Labs, D. and Neckel, H.: 1962, *Z. Astrophys.* **55**, 269.  
 Labs, D. and Neckel, H.: 1963, *Z. Astrophys.* **57**, 283.  
 Labs, D. and Neckel, H.: 1967, *Z. Astrophys.* **65**, 133.  
 Labs, D. and Neckel, H.: 1968, *Z. Astrophys.* **69**, 1.  
 Labs, D. and Neckel, H.: 1970, *Solar Phys.* **15**, 79.  
 Mankin, W. G.: 1977, in *The Solar Output and its Variation*, Colorado Assoc. Univ. Press, Boulder, p. 151.

- Moore, C. E., Minnaert, G. J., and Houtgast, J.: 1966, *The Solar Spectrum 2935 Å to 8770 Å*, Natl. Bur. Std. Monograph 61.
- Pierce, A. K.: 1954, *Astrophys. J.* **119**, 312.
- Pierce, A. K. and Slaughter, C. D.: 1977a, *Solar Phys.* **51**, 25.
- Pierce, A. K. and Slaughter, C. D.: 1977b, *Solar Phys.* **52**, 179.
- Samain, D. and Simon, P. C.: 1976, *Solar Phys.* **49**, 33.
- Thekaekara, M. P.: 1970, NASA Techn. Report TR R-351.
- Tousey, R.: 1963, *Space Sci. Rev.* **2**, 3.